CrossMark

ORIGINAL PAPER

# Estimation of actual evapotranspiration in the Nagqu river basin of the Tibetan Plateau

Mijun Zou[1] · Lei Zhong[1] · Yaoming Ma[2] · Yuanyuan Hu[1] · Lu Feng[3]

**Abstract** As a critical component of the energy and water cycle, terrestrial actual evapotranspiration (ET) can be influenced by many factors. This study was mainly devoted to providing accurate and continuous estimations of actual ET for the Tibetan Plateau (TP) and analyzing the effects of its impact factors. In this study, summer observational data from the Coordinated Enhanced Observing Period (CEOP) Asia–Australia Monsoon Project (CAMP) on the Tibetan Plateau (CAMP/Tibet) for 2003 to 2004 was selected to determine actual ET and investigate its relationship with energy, hydrological, and dynamical parameters. Multiple-layer air temperature, relative humidity, net radiation flux, wind speed, precipitation, and soil moisture were used to estimate actual ET. The regression model simulation results were validated with independent data retrieved using the combinatory method. The results suggested that significant correlations exist between actual ET and hydro-meteorological parameters in the surface layer of the Nagqu river basin, among which the most important factors are energy-related elements (net radiation flux and air temperature). The results also suggested that how ET is eventually affected by precipitation and two-layer wind speed difference depends on whether their positive or negative feedback processes have a more important role. The multivariate linear regression method provided reliable estimations of actual ET; thus, 6-parameter simplified schemes and 14-parameter regular schemes were established.

## 1 Introduction

The Tibetan Plateau (TP), with an average elevation of more than 4000 m, plays a crucial role in atmospheric circulation and global climate change due to its dynamic and thermodynamic effects (e.g., Zhong et al. 2010; Coners et al. 2016). To quantitatively understand the interaction between the land surface and the atmosphere on the TP, several field experiments have been carried out in recent decades, including the intensive observation period and long-term observation of the Global Energy and Water Cycle Experiment (GEWEX)– Asian Monsoon Experiment (GAME) on the Tibetan Plateau, (GAME/Tibet, 1996–2000) and the Coordinated Enhanced Observing Period (CEOP) Asia–Australia Monsoon Project (CAMP) on the Tibetan Plateau (CAMP/Tibet, 2001–2005) (Tanaka et al. 2001; Ma et al. 2005, 2014; Yang et al. 2010). Both GAME/Tibet and CAMP/Tibet were implemented in the Nagqu river basin in the middle of the TP, where the weather has become a little warmer and wetter from May to September every year. Previous work has found that evapotranspiration (ET), as a vital component of the hydrologic budget, returns more than 60% of precipitation on land back to the atmosphere. Also, ET is an important part of the energy balance, as vaporization of liquid water absorbs incoming terrestrial solar energy (Korzoun et al. 1978; Rosenberg et al. 1983; Nishida et al. 2003; Yao et al. 2013). However, ET is one of the most uncertain components of the water cycle, as it is difficult to estimate accurately because of the heterogeneity of the

✉ Lei Zhong
zhonglei@ustc.edu.cn

[1] Laboratory for Atmospheric Observation and Climate Environment Research, School of Earth and Space Sciences, University of Science and Technology of China, Hefei, China

[2] Key Laboratory of Tibetan Environment Changes and Land Surface Processes, Institute of Tibetan Plateau Research, the Chinese Academy of Sciences, CAS Center for Excellence in Tibetan Plateau Earth Sciences, Beijing, China

[3] Institute of Tropical and Marine Meteorology (ITMM), China Meteorological Administration (CMA), Guangzhou, China

landscape and the large number of controlling factors involved (Mu et al. 2007).

Although traditional ET observation methods (i.e., eddy correlation system, weighing lysimeter, and scintillometer) provide relatively accurate estimations of ET over a homogeneous area, these techniques are costly and difficult to maintain. At present, ET cannot be directly measured over large areas. In contrast, conventional indirect estimation methods (i.e., combinatory method and aerodynamic method), which determine ET using the surface layer gradient technique, are much easier to operate and are low cost. Therefore, these methods have been widely adopted to calculate turbulent flux (Businger et al. 1971; Li et al. 2009; Kool et al. 2014). In recent decades, remote-sensing technology has developed rapidly, providing the possibility of estimating surface ET on a larger scale (Kustas and Norman 1996; McCabe and Wood 2006; Mu et al. 2011; Chen et al. 2014). However, the quality of derived images depends very much on the complicated pre-processing (Pohl and Van Genderen 1998) and remote sensing cannot directly provide important atmospheric variables such as wind speed and vapor pressure (Kustas et al. 1994). Because of the limitations of spatial-temporal resolution, the retrieval result only represents the average conditions of each pixel and continuous monitoring is still unattainable at present. In addition, the applications of remote sensors were usually limited to cloud contamination and the biggest constraint on remote-sensing technology is the validation of retrieved ET with in situ measurements in a particular study area.

A number of analyses have been conducted on estimations of ET and its impact factors over the TP. Gu et al. (2008) pointed out that about 85% of annual ET occurs from May to September and the inter-annual variation of ET is dominated by annual precipitation. Zhang et al. (2007) compared reference ET, actual ET, and pan-evaporation across the TP and indicated that the decrease in ET is mainly contributed by a reduction in wind speed. Xue et al. (2013) estimated ET using the water balance method to evaluate four ET products for two river basins on the TP; the results showed that two ET products from Zhang et al. (2010) and Global Land Data Assimilation System with Noah Land Surface Model-2 had the best performance. Tian et al. (2013) estimated the ET in the Heihe River Basin in northwestern China based on an extended three-temperature model which was proposed by Qiu et al. (1998). The ET estimated using a three-temperature model were validated with those calculated using the water balance method. The result showed that the model could satisfy regional research requirement at large scales. Zhang et al. (2009) used multivariate linear models to determine the contributions of climate factors to ET change and found that wind speed almost predominates the changes in ET throughout the year while radiation is the leading factor in the southeast of the TP, especially in summer. Chen et al. (2006) estimated potential ET using in situ data from 101 stations on the TP and surrounding areas. The results showed that the changes in wind speed and humidity are the most important meteorological variables affecting potential ET trends on the TP, while sunshine duration plays an insignificant role.

The complex terrain and poor environmental conditions make observations difficult on the TP. Although some exploration work on ET over the TP has been carried out, no systematic research on ET has been carried out over the TP so far, among which the most imperative issues including the following: (1) the time series surface ET product for the northern TP has not been established yet; (2) there is a lack of systematic understanding of the effects of hydro-meteorological factors on ET processes on the TP. In this study, CAMP/Tibet summer observational data from 2003 to 2004 were used to determine actual summer ET (from May to September) in the Nagqu river basin using the combinatory method. Furthermore, the relationship between ET and energy factors, hydrological elements, and dynamic parameters, including multiple-layer temperature (T), relative humidity (RH), net radiation (Rn), wind speed (U), precipitation (Pre), and soil moisture (Sm), were investigated. Finally, for the convenience of application, 6-parameter simplified regression schemes and 14-parameter regular regression schemes were established and the simulation results were cross-validated with independent samples. Thus, accurate and continuous estimations of actual ET were achieved using regression schemes, which can serve as the surface validation data for remote-sensing-derived ET. Furthermore, these estimations are crucial for both quantitative understanding of land–atmosphere interactions and providing valuable information for efficient use of water resources.

# 2 Materials and methods

## 2.1 Study site

Four meteorological stations in the Nagqu river basin were selected, namely, D105, NPAM, BJ, and ANNI (Fig. 1 and Table 1). Station D105 ($33°\ 06'$ N, $91°\ 94'$ E, 5039 m) is located in the northern Nagqu river basin with flat ground and open horizons, covered by sparse alpine meadow. Station NPAM ($31°\ 93'$ N, $91°\ 72'$E, 4620 m) is covered by 15-cm-height alpine meadow. There are hills scattered 5 km to the east, 30 km to the west, and 10 km to the south and north. The ground at station BJ ($31°\ 22'$N, $91°\ 54'$E, 4509 m ) is flat and covered by low alpine meadow with high vegetation coverage. The station ANNI ($31°\ 15'$N, $92°\ 10'$ E, 4480 m), which was set up in the southeast of the station BJ, was mainly covered by sand and alpine meadow.

**Fig. 1** Locations of meteorological stations and the topography of the study area
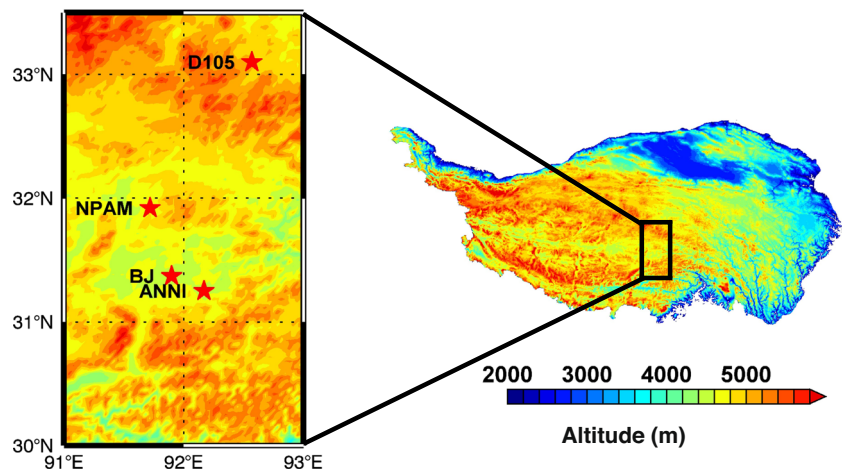


## 2.2 Datasets and measurements

The summer observational data for 2003 to 2004 from CAMP/Tibet were used in this study, which included multiple-layer temperature, relative humidity, upward shortwave radiation, downward shortwave radiation, upward longwave radiation, downward longwave radiation, wind speed, precipitation, and soil moisture. The data sampling frequency for stations D105, NPAM, and ANNI was once per hour, while that for station BJ was about every 10 min.

At stations D105 and NPAM, wind speed was measured by Komatsu. Air temperature and humidity at 9.3 and 1.0 m were measured by HMP-45D (Visala, Finland). Shortwave and longwave radiations were measured by CM11 + PIR (Kipp and Zonen, Netherlands). An automatic weather station and a planetary boundary layer tower (17 m, measuring wind speed, wind direction, air temperature, and humidity at three levels) have been installed at station ANNI. In addition, observational items also included soil moisture at six levels, soil temperature at two levels, air pressure, precipitation, turbulent flux (20 m, two levels), and radiation observations (i.e., global radiation flux, reflected radiation flux, surface longwave radiation flux, sky radiation flux) (Ma et al. 2003, 2005). Unlike the other three stations, the observed altitudes of air temperature and humidity at station BJ which is a basic observational station were 8.4 and 1.0 m, and the main measuring instruments are listed in Table 2.

## 2.3 Methods

The combinatory method was first proposed by Thom (Thom et al. 1975) and then developed by Hu (Hu et al. 1990, Hu and Qi 1991). It combines the aerodynamic method with the energy balance method. By using the universal functions of the Monin-Obukhov similarity and the surface energy balance equation, the combinatory method determines the turbulent fluxes in the surface layer. This method is independent of the specific form of Monin-Obukhov similarity; thus, the errors caused by sensing probes and the airflow disturbance from holders can be reduced. The combinatory method equations are simple at low costs and the turbulent fluxes can be derived as follows:

$$H_0 = \rho C_p k^2 Z_A^2 \frac{\partial U}{\partial Z} \frac{\partial \theta}{\partial Z} \tag{1}$$

$$\lambda ET_0 = \rho \lambda k^2 Z_A^2 \frac{\partial U}{\partial Z} \frac{\partial q}{\partial Z} \tag{2}$$

$$G_0 = G_Z + \int_0^Z C_S \frac{\partial T}{\partial t} dz \tag{3}$$

where $H_0$, $\lambda ET_0$, and $G_0$ ($W/m^2$) are the sensible heat flux, latent heat flux, and soil heat flux before correction, $\lambda$( J/kg)

**Table 2** Main instruments at station BJ

| Observation item | Instrument | Observation depth/height(m) |
|---|---|---|
| Air temperature | TS-801(Pt100) | 8.41, 1.03 |
| Wind speed | WS-D32 | 10.36, 5.02, 0.91 |
| Humidity | HMP-45D | 8.41, 1.03 |
| Air pressure | PTB220C | 0.5 |
| Precipitation | NOAH-II | 1.0 |
| Soil temperature | TS-301(Pt100) | 0.0, −0.04, −0.1, −0.2, −0.4 |
| Radiation flux | CM21、PIR | 1.25, 1.58 |
| Soil moisture | Trime EZ | −0.04, −0.2 |
| Soil heat flux | EKO | −0.4, −0.2 |

**Table 1** Average air temperature and relative humidity in summer for each meteorological station

| Station name | T(°C) | RH(%) |
|---|---|---|
| D105 | 3.64 | 62.47 |
| NPAM | 6.07 | 62.82 |
| BJ | 9.70 | 65.10 |
| ANNI | 8.08 | 64.29 |

**Table 3** Correlation coefficients between ET and different meteorological factors

| Station | U_level1 | U_level2 | U_level3 | dU | T_level1 | T_level2 | dT |
|---|---|---|---|---|---|---|---|
| D105 | 0.061[**] | 0.088[**] | 0.118[**] | 0.043[*] | 0.481[**] | 0.517[*] | 0.409[**] |
| NPAM | 0.142[**] | 0.172[**] | 0.200[**] | −0.063[**] | 0.411[**] | 0.476[**] | 0.439[**] |
| BJ | 0.040 | 0.093[**] | 0.134[**] | 0.113[**] | 0.483[**] | 0.528[**] | 0.602[**] |
| Station | RH_level1 | RH_level2 | dRH | Rn | Pre | Sm_level1 | Sm_level2 |
| D105 | -0.424[**] | −0.393[**] | 0.220[**] | 0.830[**] | −0.134[**] | 0.239[**] | 0.218[**] |
| NPAM | −0.362[**] | −0.381[**] | −0.144[**] | 0.712[**] | −0.108[**] | 0.100[**] | 0.063[**] |
| BJ | -0.531[**] | −0.540[**] | 0.004 | 0.900[**] | −0.167[**] | 0.100[**] | −0.045 |

**Correlation is significant at the 0.01 level

*Correlation is significant at the 0.05 level

is the latent heat of evaporation, $C_p$ (J/kg/K) is the specific heat capacity of air, $\rho$ ($kg/m^3$) is air density, and $k$ is the Karman constant. $Z_A = \sqrt{Z_i \cdot Z_{i+1}}$, $Z_i$ (m) and $Z_{i+1}$ (m) are the observation heights of the two levels. $G_Z(W/m^2)$ is the soil heat flux measured at a certain soil depth layer and $C_S$ is specific heat capacity of soil. $U$ (m/s) and $T$ (K) are the wind speed and air temperature, measured at a specific level. Potential temperature $\theta$ and specific humidity $q$ are defined as:

$$\theta = T\left(\frac{1000}{P}\right)^{0.286} \tag{4}$$

$$q = \frac{0.622e}{P-0.378e} \tag{5}$$

where P (hPa) is atmospheric pressure and $e$ (hPa) is water vapor pressure.

$$F = \frac{R_n-G_0}{H_0 + \lambda E_0} \tag{6}$$

$$\lambda ET = \lambda ET_0 \cdot F \tag{7}$$

where $F$ is the stratification influence function, $\lambda ET$ ($W/m^2$) is the latent heat flux after correction, and ET (mm) is evapotranspiration. The constant settings were as follows:

$k = 0.4$

$C_p = 1004.07$ J/(kg·K)

$\lambda = 2.45^*10^6$ J/kg

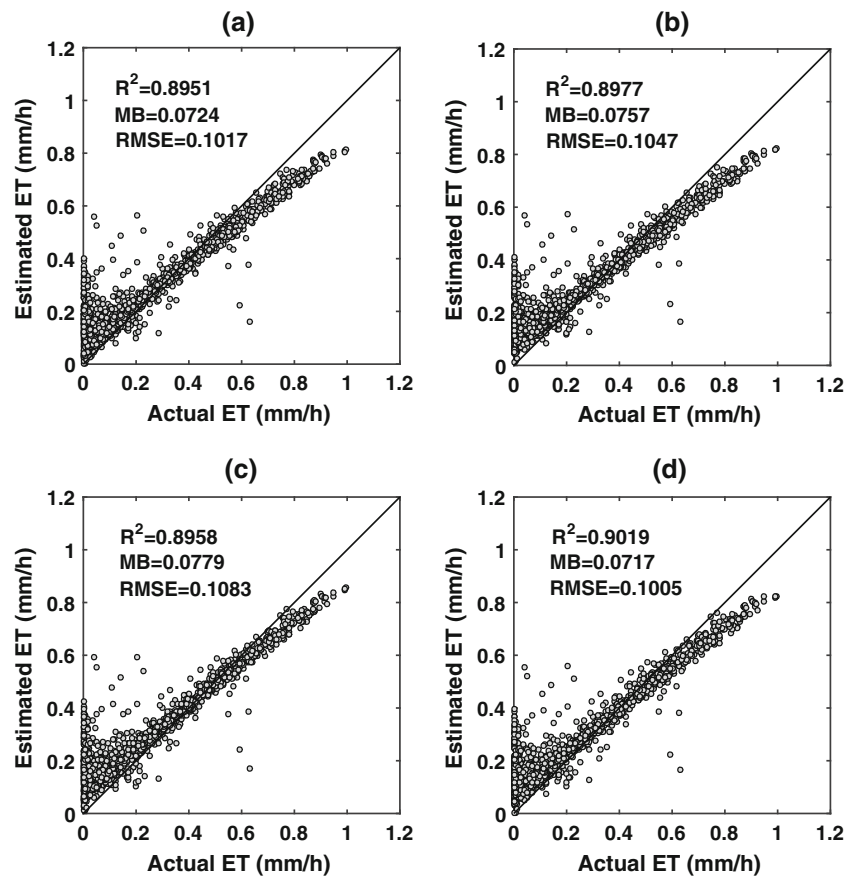$\rho = 1.293$ kg/$m^3$

$C_S = 1.18 \times 10^6$ J/(m$^3$·K)

In this study, the input data which were beyond the valid range (i.e., temperature $-50 \sim 50$ °C; relative humidity: $0 \sim 1$; four radiation components, wind speed, precipitation, and soil moisture must be larger than 0), were treated as outliers. To ensure the quality of ET data, the data were sorted from small to large and those values within the range of 0 mm to the threshold at 0.05 significant level were selected. The outliers and diverging data were eliminated during the data processing. The main work of this study consisted of the following aspects.

(1) The outliers were eliminated by taking valid ranges and temporal continuity into account.
(2) For station BJ, the 10-min interval data were aggregated into 60-min interval data.

**Table 4** Expressions of the four optimum schemes (14-parameter cases)

| Scheme | Variables | Expression |
|---|---|---|
| 1 | U1, U5, T1, T2, RH1, RH2, Pre, Sm4, Sm10, Rn | y = −0.0565 + 0.0324*U1–0.0376*U5 + 0.0850*T1–0.0801*T2–0.0066*RH1 + 0.0072*RH2–0.0136*Pre-0.0011*Sm4 + 0.0012*Sm10 + 0.0009*Rn |
| 2 | U1, U5, T1, T2,RH1, RH2, Sm4, Sm10, Rn | y = −0.0533 + 0.0320*U1–0.0372*U5 + 0.0853*T1–0.0804*T2–0.0067*RH1 + 0.0073*RH2–0.0011*Sm4 + 0.0013*Sm10 + 0.0009*Rn |
| 3 | U5, dU, T1, T2, RH1, RH2, Sm4, Sm10, Rn | y = −0.0446–0.0094*U5–0.0213*dU + 0.0835*T1–0.0787*T2–0.0069*RH1 + 0.0074*RH2–0.0012*Sm4 + 0.0014*Sm10 + 0.0009*Rn |
| 4 | U1, U5, T1, T2, dRH, Sm4, Sm10, Rn | y = −0.0147 + 0.0311*U1–0.0366*U5 + 0.0860*T1–0.0816*T2 + 0.0062*dRH-0.0009*Sm4 + 0.0014*Sm10 + 0.0009*Rn |

**Fig. 2** Validation of the four optimum model simulation results in summer 2004 (14-parameter cases; **a–d** represent Scheme 1, Scheme 2, Scheme 3 and Scheme 4, respectively)



(a) $R^2=0.8951$, MB=0.0724, RMSE=0.1017

(b) $R^2=0.8977$, MB=0.0757, RMSE=0.1047

(c) $R^2=0.8958$, MB=0.0779, RMSE=0.1083

(d) $R^2=0.9019$, MB=0.0717, RMSE=0.1005

(3) ET was determined using the combinatory method and diverging data were eliminated from the results.

(4) The correlation coefficients of ET were calculated (after abnormal values were eliminated) using the regression model. On this basis, the effects of the impact factors on ET were analyzed.

(5) Based on summer in situ hourly data at stations D105, NPAM, and BJ, different linear regression models were set up to simulate ET. The models were divided into 6-parameter cases and 14-parameter cases. All models were established by assembling the different parameters. The results were then compared with those from step (3).

(6) Four optimum schemes were selected and validated using station ANNI summer ET in 2004. The simulation scheme results were inter-compared.

**Table 5** Comparison between the four optimum model simulation results and actual ET at station ANNI (14-parameter case)

| Scheme | $R$ | MB | RMSE |
|---|---|---|---|
| 1 | 0.9442 | 0.0724 | 0.1017 |
| 2 | 0.9455 | 0.0757 | 0.1047 |
| 3 | 0.9445 | 0.0779 | 0.1083 |
| 4 | 0.9479 | 0.0717 | 0.1005 |

## 3 Results and discussion

### 3.1 Analyses of impact factors

ET is mainly constrained by three aspects: energy, water vapor transport conditions, and water supply capacity of the medium. Factors analysis was performed by taking 14 meteorological parameters into account, including three-level wind speed (U_level1, U_level2, U_level3; U1, U2, U3 for short, respectively), two-level air temperature (T_level1, T_level2; T1, T2 for short), two-level humidity (RH_level1, RH_level2; RH1, RH2 for short), net radiation (Rn), precipitation (Pre), two-layer soil moisture (Sm_level1, Sm_level2; Sm1, Sm2 for short), two-layer wind speed difference (dU), two-layer air temperature difference (dT), and two-layer humidity difference (dRH). Table 3 provides the details of the correlation coefficients between ET and the 14 related parameters. The observation heights of three-level wind speed were 1, 5, and 10 m. The observation height of T1 and RH1 was 1.0 m, while the height for T2 and RH2 was 9.3 m (except at station BJ where it was 8.4 m). The observation heights of Sm1 and Sm2 were 4 and 20 cm. dU is the difference in wind speed between U3 and U1. dT and

**Table 6** Expressions of the four optimum schemes (6-parameter cases)

| Scheme | Variables | Expression |
|--------|-----------|------------|
| 1 | T, RH, Pre, Sm, Rn | y = 0.1035 + 0.0013*T-0.0002*RH-0.0270*Pre + 0.0008*Sm + 0.0006*Rn |
| 2 | U, RH, Pre, Sm, Rn | y = 0.1276–0.0034*U-0.0004*RH-0.0256*Pre + 0.0009*Sm + 0.0006*Rn |
| 3 | U, T, Pre, Sm, Rn | y = 0.1009–0.0032*U + 0.0018*T-0.0284*Pre + 0.0006*Sm + 0.0006*Rn |
| 4 | U, T, RH, Pre, Sm, Rn | y = 0.1225–0.0036*U + 0.0015*T-0.0003*RH-0.0259*Pre + 0.0007*Sm + 0.0006*Rn |

dRH are the difference between T2 and T1 and between RH2 and RH1, respectively.

The main results from Table 3 are as follows. (1) The correlation coefficients between ET and three-level wind speed were all positive. This is due to an increase in wind speed accelerating the transfer of water molecules. The correlation coefficient for 10-m wind speed was the highest while that for 1-m wind speed was the lowest of the three levels. (2) On one hand, an increase in dU can expedite the interaction between the land surface and atmosphere thus resulting in ET enhancement. On the other hand, an increase in dU can enhance sensible heat while reducing latent heat. The positive correlation at stations D105 and BJ (with correlation coefficients of 0.043 and 0.113) meant that the eventual impact of dU on ET was mainly dominated by an acceleration of the land surface–atmosphere interaction. In contrast, a negative correlation at station NPAM (with a correlation coefficient of −0.063) meant that the eventual impact of dU on ET was mainly dominated by enhancement of sensible heat flux and reduction of latent heat flux. (3) For T, all stations showed strong positive correlations with ET. T is an important element representing energy supply. Higher T results in a higher ratio of the energy used for ET coming from absorbed solar energy (Gu et al. 2008). (4) For dT, stations D105, NPAM and BJ showed strong positive correlations with ET (with correlation coefficients of 0.409, 0.439, and 0.602), indicating that an increase in dT contributes to the unstable stratification and accelerates ET. (5) The strong negative correlations between ET and RH suggested that wet air reduces ET because of the smaller moisture difference between the air and soil. (6) The significant positive correlation between ET and Rn (with correlation coefficients of 0.830, 0.712, and 0.900 for stations D105, NPAM, and BJ, respectively) implied that the more energy the land surface receives, the more sufficient the energy supply is. In humid regions, energy is more important for ET than water supply

(Liu et al. 2010). (7) Similar to dU, the effects of Pre on ET were twofold. Although precipitation enhances surface water supply capability, the increasing air humidity reduces ET at the same time. The negative correlations (with correlation coefficients of −0.134, −0.108, and −0.167 for station D105, NPAM, and BJ, respectively) showed that the eventual impact of Pre was mainly dominated by a reduction of ET in the Nagqu river basin. (8) As a direct reflection of surface water supply capability, the more soil moisture, the more water is available for ET. Sm was positively correlated with ET in the shallow layer (with correlation coefficients of 0.239, 0.100, and 0.100 for stations D105, NPAM, and BJ, respectively), while the deeper layer showed a weak correlation at stations D105 and NPAM (with correlation coefficients of 0.218 and 0.063) and no correlation at station BJ.

In summary, there were significant correlations between ET and the selected hydro-meteorological factors in the Nagqu river basin. The most important factors were energy-related elements (net radiation and air temperature). It can be concluded that in summer, when water supply is sufficient, energy is the main limiting factor for ET. However, how ET is eventually affected by dU and Pre depends on whether their positive or negative feedbacks have a more important role.

### 3.2 Regression scheme analysis

First, the 14 meteorological parameters were chosen as regressors. The summer data for stations D105, NPAM, and BJ from 2003 to 2004 at 60-min intervals were used to build the regression models. Then, the model results were validated using station ANNI summer ET in 2004. All linear regression models were established by assembling the different hydro-meteorological parameters and the model results were compared with ET derived using the combinatory method. Four optimum schemes were selected on the basis of (1) minimum residual of the regression model and (2) all regressors being significant. The details of the four optimum schemes are listed in Table 4.

Figure 2 shows the validation results for the four optimum 14-parameter regular schemes. The x- and y-axes represent actual ET and model-simulated ET. The black solid lines are the 1:1 line. The results showed that the four optimum

**Table 7** Comparison between the four optimum model simulation results and actual ET at station ANNI (6-parameter cases)

| Scheme | R | MB | RMSE |
|--------|------|--------|--------|
| 1 | 0.9669 | 0.0879 | 0.1082 |
| 2 | 0.9643 | 0.0882 | 0.1100 |
| 3 | 0.9647 | 0.0977 | 0.1393 |
| 4 | 0.9654 | 0.0878 | 0.1079 |

**Fig. 3** Validation of the four optimum model simulation results in summer 2004 (6-parameter cases; **a**–**d** represent Scheme 1, Scheme 2, Scheme 3 and Scheme 4, respectively)
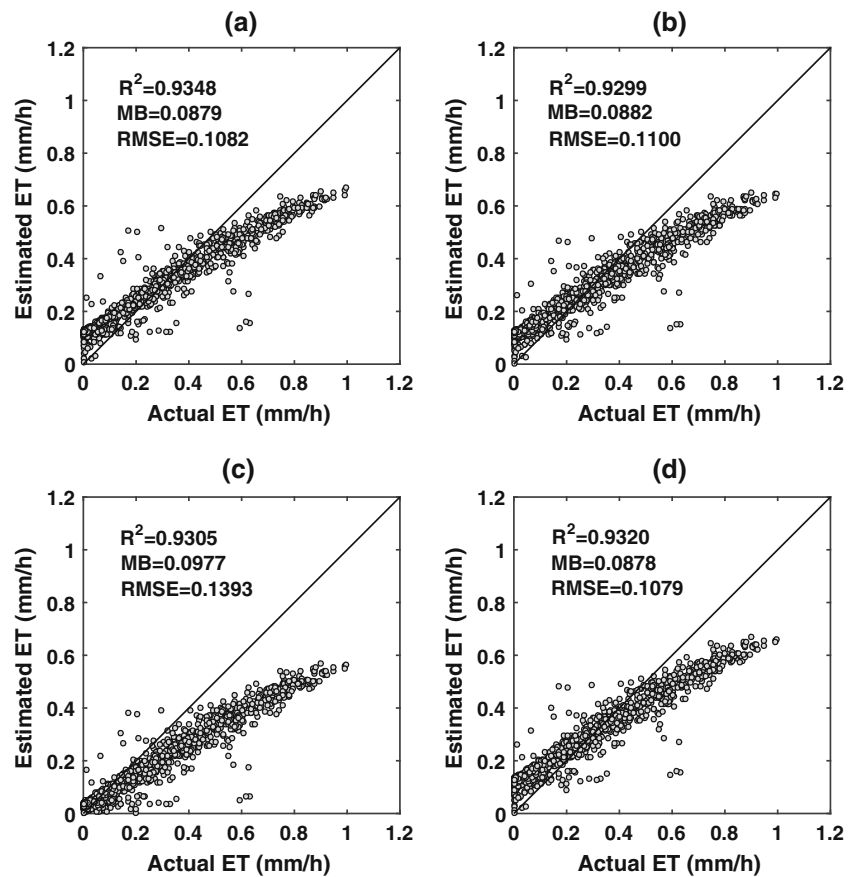


schemes fit well to the actual ET, although some overestimation occurred when ET < 0.05 and some underestimation occurred when ET was relatively high.

Table 5 provides the details of the validation results, which consists of the correlation coefficient ($R$), mean bias (MB) and root-mean-square error (RMSE). Among the four optimum schemes, Scheme 4 performed best with the highest $R$ and lowest RMSE of 0.948 and 0.101.

For the convenience of application, the involved regressors were reduced to six parameters: wind speed (U, the average of three-layer wind speed), air temperature (T, the average of two-layer air temperature), relative humidity (RH, the average of two-layer relative humidity), precipitation (Pre), net radiation (Rn), and soil moisture (Sm, the average of two-layer soil moisture). Similarly, four optimum schemes were built by taking the residual of the regression estimations, significant regressors, and goodness of fit into account. The regressors used to build the four optimum schemes are shown in Table 6.

As can be seen from the validation results for the 6-parameter cases (Table 7), among the four optimum schemes, Scheme 1 performed best followed by Scheme 4, with $R = 0.967$ and 0.9654, and RMSE = 0.1082 and 0.1079, respectively.

Figure 3 shows the validation results for the four optimum 6-parameter simplified schemes. The results showed that the four optimum schemes fit well to actual ET, except for Scheme 3, which underestimated ET when ET was relatively high. Compared with the 14-parameter cases, the overestimation at low ET values was improved. Accordingly, when taking only six parameters into account, Scheme 1 and Scheme 4 can be applied in practical work.

# 4 Conclusion

In this study, summer in situ data from 2003 to 2004 were used to determine actual ET and investigate its relationship with multiple-layer temperature, relative humidity, net radiation flux, wind speed, precipitation, and soil moisture. The effects of meteorological and hydrological factors on ET for the Nagqu river basin were elaborated. For the convenience of application, 6-parameter and 14-parameter ET estimation models were built, in which four optimum schemes were selected by taking the minimum residual of the regression estimations, significant regressors and goodness of fit into account. The validation of the simulation results with actual ET showed good agreement. From this study, the following conclusions were drawn.

(1)  There were significant correlations between actual ET of the Nagqu river basin and most of the selected hydro-meteorological parameters. The most significant correlation was found with energy-related elements (net radiation and air temperature).

(2)  How ET was eventually affected by precipitation and two-layer wind speed difference depended on whether their positive or negative feedback processes had a more important role.

(3)  When 14 parameters were used in the regression models, the four optimum schemes corresponded well with actual ET, although some overestimation occurred when ET < 0.05. The simulation results for Scheme 4 performed best, with $R = 0.9479$ and RMSE = 0.1005.

(4)  When six parameters were used to build the ET models, the four optimum schemes fitted well to actual ET and the overestimation at low ET values was improved. The simulation results for Scheme 1 performed best, followed by Scheme 4, with $R = 0.9669$ and 0.9654, and RMSE = 0.1082 and 0.1079, respectively.

However, the calculation results are sensitive to observation error and there exist some calculation stability problems for the combinatory method, that is, when the ratio of $H_0$ to $\lambda ET_0$ is close to $-1$, ET would be divergent and show some inauthentic crest value. In future work, more parameters (i.e., soil properties) will be taken into account to further improve the models which require more precise and comprehensive measurements over the TP.

# References

Businger JA, Wyngaard JC, Izumi Y (1971) Bradley EF 1971 flux-profile relationships in the atmospheric surface layer. J Atmos Sci 28(2): 181–189

Coners H, Babel W, Willinghöfer S, Biermann T, Köhler L, Seeber E, Foken T, Ma YM, Yang YP, Miehe G, Leuschner C (2016) Evapotranspiration and water balance of high-elevation grassland on the Tibetan Plateau. J Hydrol 533:557–566

Chen S, Liu Y, Thomas A (2006) Climatic change on the Tibetan Plateau: potential evapotranspiration trends from 1961–2000. Clim Chang 76(3–4):291–319. doi:10.1007/s10584-006-9080-z

Chen Y, Xia J, Liang S et al (2014) Comparison of satellite-based evapotranspiration models over terrestrial ecosystems in China. Remote Sens Environ 140:279–293

Tian F, Qiu GY, Yang YH, Lu YH, Xiong Y (2013) Estimation of evapotranspiration and its partition based on an extended three-temperature model and MODIS products. J Hydrol 498:210–220

Gu S, Tang YH, Cui XY, Du MY, Zhao L, Li YN, Xu SX, Zhou HK, Kato T, Qi PT, Zhao XQ (2008) Characterizing evapotranspiration over a meadow ecosystem on the Qinghai-Tibetan Plateau. J Geophys Res-Atmos 113(D8). doi:10.1029/2007JD009173

Hu YQ, Qi YJ, Yang XL (1990) Preliminary analyses about characteristics of microclimate and heat energy budget in hexi gobi (Huayin). Plateau Meteorology 2:001 (In Chinese)

Hu YQ, Qi YJ (1991) Combinatory method to determine the turbulent fluxes and the universal functions in the surface layer. Acta Meteorologica Sinica 49(001):46–53 (In Chinese)

Kool D, Agam N, Lazarovitch N, Heitman JL, Sauer TJ, Ben-Gal A (2014) A review of approaches for evapotranspiration partitioning. Agric For Meteorol 184:56–70

Korzoun VI, Sokolov AA, Budyko MI, Voskresensky KP, Kalininin GP, Konoplyanstev AA, KorotkevichES, Kuzin PS, Lvovich MI (eds) (1978) World water balance and water resources of the earth. UNESCO, Paris

Kustas WP, Perry EM, Doraiswamy PC et al (1994) Using satellite remote sensing to extrapolate evapotranspiration estimates in time and space over a semiarid rangeland basin. Remote Sens Environ 49(3): 275–286

Kustas WP, Norman JM (1996) Use of remote sensing for evapotranspiration monitoring over land surfaces. Hydrol Sci J 41(4):495–516

Li ZL, Tang RL, Wan ZM, Bi YY, Zhou CH, Tang BH, Yan GJ, Zhang XY (2009) A review of current methodologies for regional evapotranspiration estimation from remotely sensed data. Sensors 9(5): 3801–3853. doi:10.3390/s90503801

Liu B, Xiao ZN, Ma ZG (2010) Relationship between pan evaporation and actual evaporation in different humid and arid regions of China. Plateau Meteorology 29(3):629–636 (In Chinese)

Ma YM, Su ZB, Koike T, Yao TD, Ishikawa H, Ueno K, Menenti M (2003) On measuring and remote sensing surface energy partitioning over the Tibetan Plateau—from GAME/Tibet to CAMP/Tibet. Phys Chem Earth Parts A/B/C 28(1):63–74. doi:10.1016/S1474-7065(03)00008-1

Ma YM, Fan S, Ishikawa H, Tsukamoto O, Yao T, Koike T, Zuo H, Su ZB (2005) Diurnal and inter-monthly variation of land surface heat fluxes over the central Tibetan Plateau area. Theor Appl Climatol 80(2–4):259–273. doi:10.1007/s00704-004-0104-1

Ma YM, Zhu ZK, Zhong L, Wang BB, Han CB, Wang Z, Wang Y, Lu L, Amatya PM, Ma W, Hu Z (2014) Combining MODIS, AVHRR and in situ data for evapotranspiration estimation over heterogeneous landscape of the Tibetan Plateau. Atmos Chem Phys 14(3):1507–1515. doi:10.5194/acp-14-1507-2014

McCabe MF, Wood EF (2006) Scale influences on the remote estimation of evapotranspiration using multiple satellite sensors. Remote Sens Environ 105(4):271–285. doi:10.1016/j.rse.2006.07.006

Mu Q, Heinsch FA, Zhao M, Running SW (2007) Development of a global evapotranspiration algorithm based on MODIS and global meteorology data. Remote Sens of Environ 111(4):519–536. doi:10.1016/j.rse.2007.04.015

Mu Q, Zhao M, Running SW (2011) Improvements to a MODIS global terrestrial evapotranspiration algorithm. Remote Sens Environ 115(8):1781–1800. doi:10.1016/j.rse.2011.02.019

Nishida K, Nemani RR, Glassy JM, Running SW (2003) Development of an evapotranspiration index from Aqua/MODIS for monitoring surface moisture status. IEEE Trans Geosci Remote Sens 41(2):493–501. doi:10.1109/TGRS.2003.811744

Pohl C, Van Genderen JL (1998) Review article multisensor image fusion in remote sensing: concepts, methods and applications. Int J Remote Sens 19(5):823–854. doi:10.1080/014311698215748

Qiu GY, Yano T, Momii K (1998) An improved methodology to measure evaporation from bare soil based on comparison of surface temperature with a dry soil surface. J Hydrol 210(1):93–105

Rosenberg NJ, Blad BL, Verma SB (1983) Microclimate: the biological environment. John Wiley & Sons

Tanaka K, Ishikawa H, Hayashi T, Tamagawa I, Ma Y (2001) Surface energy budget at Amdo on the Tibetan Plateau using GAME/Tibet IOP98 data. J Meteor Soc Japan 79:505–517

Thom AS, Stewart JB, Oliver HR, Gash JHC (1975) Comparison of aerodynamic and energy budget estimates of fluxes over a pine forest. Quart J Roy Meteor Soc 101(427):93–105

Xue BL, Wang L, Li XP, Yang K, Chen DL, Sun LT (2013) Evaluation of evapotranspiration estimates for two river basins on the Tibetan Plateau by a water balance method. J Hydrol 492:290–297

Yang K, He J, Tang WJ, Qin J, Cheng CCK (2010) On downward shortwave and longwave radiations over high altitude regions: observation and modeling in the Tibetan Plateau. Agric For Meteorol 150(1):38–46. doi:10.1016/j.agrformet.2009.08.004

Yao YJ, Liang SL, Cheng J, Liu SM, Fisher JB, Zhang XD, Jia K, Zhao X, Qin Q, Zhao B, Han SJ, Zhou GS, Zhou GY, Li YL, Zhao SH (2013) MODIS-driven estimation of terrestrial latent heat flux in China based on a modified Priestley–Taylor algorithm. Agric For Meteorol 171:187–202

Zhang K, Kimball JS, Nemani RR, Running SW (2010) A continuous satellite-derived global record of land surface evapotranspiration from 1983 to 2006. Water Resour Res 46(9). doi:10.1029/2009WR008800

Zhang Y, Liu C, Tang Y, Yang Y (2007) Trends in pan evaporation and reference and actual evapotranspiration across the Tibetan Plateau. J Geophys Res-Atmos 112(D12). doi:10.1029/2006JD008161

Zhang X, Ren Y, Yin ZY, Lin Z, Du Z (2009) Spatial and temporal variation patterns of reference evapotranspiration across the Qinghai-Tibetan Plateau during 1971–2004. J Geophys Res-Atmos 114(D15). doi:10.1029/2009JD011753

Zhong L, Ma Y, Salama MS, Su Z (2010) Assessment of vegetation dynamics and their response to variations in precipitation and temperature in the Tibetan Plateau. Clim Chang 103:519–535. doi:10.1007/s10584-009-9787-8